Cubature and Quadrature based Continuous-discrete Filters for Maneuvering Target Tracking

Abhinoy Kumar Singh
Dept. of Biomedical Engg.
Mcgill University, Montreal,
Quebec, Canada
abhinoy@iitp.ac.in

Kundan Kumar
Dept. of Electrical Engg.
IIT Patna,
Patna, India
kundan.pee16@iitp.ac.in

Swati
Dept. of Electrical Engg.
IIT Patna,
Patna, India
swati_iitp@iitp.ac.in

Shovan Bhaumik
Dept. of Electrical Engg.
IIT Patna,
Patna, India
shovan.bhaumik@iitp.ac.in

***Abstract*—A continuous-discrete system represents a system with continuous process and discrete measurement models. Very recently, two filters namely cubature quadrature Kalman filter (CQKF) and Gauss-Hermite filter (GHF) are introduced to solve the filtering problems for discrete-time systems where both the process and measurement models are discrete in nature. In this paper we extend the two estimators so that they could work for continuous process and discrete measurement model. The proposed filters are applied to solve a continuous-discrete maneuvering air-traffic-control problem and the results are compared with continuous-discrete Kalman filter (CD-CKF) in terms of the root mean square error (RMSE). It has been found that the proposed methods provide better estimation accuracy compared to the CD-CKF.**

***Index Terms*—Continuous-discrete system, cubature quadrature Kalman filter, Gauss-Hermite filter**

I. Introduction

Filtering is a recursive process of state estimation of a dynamic system. It is commonly applicable in many real-life problems like target tracking [1]–[3], navigation [4], systems identification [5] *etc.*, to name a few. In nonlinear filtering literature, the discrete-time filters are popular and a wide variety of them are available [1], [6]–[11]. In discrete-time systems, both the process and measurements are in discrete-time domain while in reality often the process is described in continuous domain. Such systems where the process is described in continuous and measurement is in discrete domain are called continuous-discrete systems.

Generally, for filtering purpose the designer discretizes the plant at sampling interval and treats a continuous-discrete system as a discrete-time system. The discretization accounts for additional approximation that may cause for inaccuracy. To get rid of this, few notable filters, namely the continuous-discrete extended Kalman filter (CD-EKF) [12], [13], the continuous-discrete unscented Kalman filter (CD-UKF) [14], the continuous-discrete cubature Kalman filter (CD-CKF) [15] *etc.* have been introduced. The motivation of this paper is to further improve the filtering accuracy of the continuous-discrete systems.

The recently introduced discrete-time filters, with deterministic sample points, could be divided into two parts; cubature based and quadrature based filters. Major cubature based filters available in literature are cubature Kalman filter (CKF) [7], cubature quadrature Kalman filter (CQKF) [8], higher-degree cubature Kalman filter (HDCKF) [9] and higher-degree cubature quadrature Kalman filter (HDCQKF) [10], while the major quadrature based filters are Gauss-Hermite filter (GHF) [16], [17] and sparse-grid Gauss-Hermite filter (SGHF) [18], [19]. In this paper, we explore the possibility of developing continuous-discrete version of the above mentioned filters.

To perform the continuous-discrete filtering, the process model is first discretized over the sampling period. The discretization is performed in two steps. In the first step, the ordinary differential equation (ODE) is obtained by implementing the Fokker-Planck equation to the given continuous model. However, in the second step, the discretized model is obtained by applying Itô-Taylor expansion of order 1.5 over the ODE. As soon as the model is discretized, the filtering problem reduces to the approximation of intractable integrals of the form *nonlinear function*$\times$*normal distribution*, similar to the ordinary nonlinear filtering problems.

During the implementation of continuous-discrete filtering algorithms, many times complex matrix inversions are performed which causes numerical instability. To omit this instability, the square-root extension is used in this paper. But during the square-root filtering, the square-root of weights are computed which needs positive weight certainty for all the sample points. Consequently, the HDCKF, the HDCQKF and the SGHF are discarded from this extension as many sample points have negative weight in these filters. Hence the major contribution of this paper is to enhance the conventional CQKF and GHF algorithms to deal with the continuous-discrete systems in order to enhance their filtering accuracy. Also, a brief explanation is provided at the end of this paper to estimate the initial covariance of target and measurement noise covariance. In this paper, we explore the possibility of developing continuous-discrete version of the above mentioned filters.

The remaining part of the paper is organized as follow: The continuous-discrete filtering problem is formulated in section-II, which is followed by section-III where the filtering procedure for such problems are described. In section-IV, the numerical approximation methods used to approximate the intractable integrals in the proposed filters are discussed.

978-0-9964527-7-9 ©2018 ISIF

The filters are simulated to solve a continuous-discrete maneuvering target tracking problem in section-V and finally, the discussions and conclusions are drawn in section-VI. In appendices, the algorithm for implementation is discussed and also a method is derived to formulate the initial covariance and noise error covariance.

II. Problem formulation

Let us consider a state space model with continuous process equation, given as [14], [15]

$$dx(t) = f(x(t), t)dt + \sqrt{Q}d\beta(t), \tag{1}$$

where $x(t)$ is an n-dimensional state of a continuous-discrete system at any time t, $f(\cdot)$ is called drift function and $Q \in \Re^{n\times n}$ is called diffusion matrix. $\beta(t)$ is an n-dimensional standard Wiener process with increment $d\beta(t)$.

The noisy measurements received at time instants $t_k = kT$ (T is measurement sampling interval) is

$$y_k = \gamma(x_k) + v_k, \tag{2}$$

where $y_k \in \Re^d$ is the measurement at k^{th} time instant, $\gamma(\cdot)$ is a nonlinear function and measurement noise $v_k \in \Re^d$ is assumed to be Gaussian with zero mean and known covariance R.

We assume $f(\cdot)$ to be at least twice differentiable with respect to x and at least once differentiable with respect to t. γ is assumed to be at least once integrable with respect to normal density. These assumptions are easily satisfied in many engineering applications including tracking, which is the main focus of our paper.

In this paper, the filtering under Bayesian framework is adopted which is performed in two steps:

1) *Prediction step:* This step involves the computation of prior probability density function using the Chapman-Kolmogorov equation,
$$p(x_k|y_{1:k-1}) = \int p(x_k|x_{k-1})p(x_{k-1}|y_{1:k-1})dx_{k-1}. \tag{3}$$
2) *Update step:* In this step, the posterior probability density function is evaluated using the Baye's rule,
$$p(x_k|y_{1:k}) = \frac{p(y_k|x_k)p(x_k|y_{1:k-1})}{p(y_k|y_{1:k-1})}, \tag{4}$$
where the normalizing constant
$$p(y_k|y_{1:k-1}) = \int p(y_k|x_k)p(x_k|y_{1:k-1})dx_k. \tag{5}$$

The integrals appeared in Eqs. (3)-(5) are intractable for most of the nonlinear systems. With Gaussian assumption of the conditional pdfs, the integrals reduce to the form of *nonlinear function*×*normal distribution* which is mostly intractable. During the filtering, these intractable integrals are approximated numerically.

III. Bayesian framework of filtering for continuous-discrete systems

Before proceeding forward to the continuous-discrete filtering, the process model is discretized at a smaller scale than the sampling interval.

A. Discretization of Process Model

The discretization procedure involves two steps. In the first step, the process model is reduced to a stochastic ODE by using Fokker-Planck equation while in the second step the stochastic ODE is reduced to an ordinary discrete equation.

1) Reduction of continuous system to stochastic ODE: Using the Fokker-Planck equation, at any time t *i.e.* $t_k < t < t_{k+1}$, the conditional density of $x(t)$ *i.e.* $p(x_t|y_{1:k})$ satisfies the following differential equation [14], [15]

$$\begin{aligned}\frac{\partial p(x_t|y_{1:k})}{\partial t} =& -\sum_{i=1}^{n}\frac{\partial}{\partial \mathsf{x}_i}[f_i(x(t),t)p(x_t|y_{1:k})] \\ &+ \sum_{i=1}^{n}\sum_{j=1}^{n}\frac{\partial^2}{\partial \mathsf{x}_i \partial \mathsf{x}_j}[D_{ij}p(x_t|y_{1:k})],\end{aligned} \tag{6}$$

where x_i is the i^{th} element of x and $D_{ij} = \frac{1}{2}\sum_{l=1}^{n}\sqrt{Q}_{il}\sqrt{Q}_{jl}$ is diffusion tensor.

2) Reduction of stochastic ODE to discrete model: In this step, the stochastic ODE appeared in Eq. (6) is approximated and a linear process model is derived. In filtering literature, this approximation has been performed using two different approaches, namely the Euler method and the Itô-Taylor expansion of order 1.5. The Euler method was used in early approaches, *viz.* the CD-EKF [12] and the CD-UKF [14]. Later, in CD-CKF this method was replaced by Itô-Taylor expansion of order 1.5 and claimed that the Euler method is equivalent to the Itô-Taylor expansion of order 0.5 which is comparatively less accurate. By using the Itô-Taylor expansion of order 1.5 over time interval $(t, t+\delta)$, the stochastic ODE Eq. (6) could be reduced to [15]

$$\begin{aligned}x(t+\delta) =& x(t) + \delta f(x(t),t) + \frac{1}{2}\delta^2(\mathbb{L}_0 f(x(t),t)) \\ &+ \sqrt{Q}\mathtt{w} + (\mathbb{L}f(x(t),t))q,\end{aligned} \tag{7}$$

where

$$\mathbb{L}_0 = \frac{\partial}{\partial t} + \sum_{i=1}^{n} f_i\frac{\partial}{\partial x_i} + \frac{1}{2}\sum_{j,p,q=1}^{n}\sqrt{Q}_{p,j}\sqrt{Q}_{q,j}\frac{\partial^2}{\partial x_p \partial x_q}$$

$$\text{and} \quad \mathbb{L} = \sum_{j,i=1}^{n}\sqrt{Q}_{i,j}\frac{\partial}{\partial x_i}.$$

We can consider

$$f_d(x(t),t) = x(t) + \delta f(x(t),t) + \frac{1}{2}\delta^2(\mathbb{L}_0 f(x(t),t)) \tag{8}$$

as noise free process function. The process noise is given by n-dimensional correlated Gaussian random variables, $(\mathtt{w}, q)$, which are independent of state vector $x(t)$ and distributed with zero mean and covariance matrices

$$\mathbb{E}[\mathtt{w}\mathtt{w}^T] = \delta I_n, \;\; \mathbb{E}[\mathtt{w}q^T] = \frac{1}{2}\delta^2 I_n, \;\; \text{and} \;\; \mathbb{E}[qq^T] = \frac{1}{3}\delta^3 I_n.$$

After discretizing the process equation, an m-step iterations of length δ is performed over the time interval T ($t_k - t_{k-1} = T = m\delta$), for computing the predicted state and its error covariance (in *time update*). To this regard, m number of

intermediate steps are considered between two samples. Then, the filtering of continuous-discrete systems is performed in two steps; prediction step and update step.

B. Prediction Step

Let us assume, $x^j_{k-1|k-1}$ denotes an intermediate state of a dynamic target at time $t = (k-1)T + j\delta;\ 1 \leq j \leq m$. Then the predicted state estimate at time t can be given as

$$\begin{aligned}\hat{x}^j_{k-1|k-1} &= \mathbb{E}[x^j_{k-1}|y_{1:k-1}] = \mathbb{E}[f_d(x_{k-1},(k-1)T)|y_{1:k-1}] \\ &= \int f_d(x_{k-1},(k-1)T)\aleph(x_{k-1};\hat{x}_{k-1|k-1}, \\ &\quad P_{k-1|k-1})dx_{k-1}.\end{aligned} \tag{9}$$

Similarly, the predicted state-error covariance matrix can be given as

$$\begin{aligned}&P^j_{k-1|k-1} \\ &= \mathbb{E}[(x^j_{k-1} - \hat{x}^j_{k-1|k-1})(x^j_{k-1} - \hat{x}^j_{k-1|k-1})^T|y_{1:k-1}] \\ &= \mathbb{E}[(f_d(\cdot) + \sqrt{Q}\mathtt{w} + \mathbb{L}f(\cdot)q - \hat{x}^j_{k-1|k-1})(f_d(\cdot) + \sqrt{Q}\mathtt{w} \\ &+ \mathbb{L}f(\cdot)q - \hat{x}^j_{k-1|k-1})^T|y_{1:k-1}] \\ &= \int f_d(\cdot)f_d(\cdot)^T\aleph(\cdot)dx_{k-1} + \frac{\delta^3}{3}\int \mathbb{L}f(\cdot)\mathbb{L}f(\cdot)^T\aleph(\cdot)dx_{k-1} \\ &+ \frac{\delta^2}{2}\Big[\sqrt{Q}\Big(\int \mathbb{L}f(\cdot)\aleph(\cdot)\Big)^T + \Big(\int \mathbb{L}f(\cdot)\aleph(\cdot)dx_{k-1}\Big)\sqrt{Q}^T \\ &- (\hat{x}^j_{k-1|k-1})(\hat{x}^j_{k-1|k-1})^T + \delta Q.\end{aligned} \tag{10}$$

Here $f_d(x_{k-1},(k-1)T)$, $f(x_{k-1},(k-1)T)$ and $\aleph(x_{k-1};\hat{x}_{k-1k-1}, P_{k-1k-1})$ are represented by $f_d(\cdot)$, $f(\cdot)$ and $\aleph(\cdot)$ respectively. At the end, we make an assumption that $\mathbb{E}[\mathbb{L}f(x_{k-1},(k-1)T)] \approx \mathbb{L}f(\hat{x}^{j-1}_{k-1|k-1},(k-1)T)$. This approximation does not affect the accuracy much until the nonlinearity of $\mathbb{L}f(\cdot)$ is not severe.

To find the predicted state estimate $\hat{x}_{k|k-1}$ and error covariance $P_{k|k-1}$, $\hat{x}^j_{k-1|k-1}$ and $P^j_{k-1|k-1}$ are approximated successively until j reaches to m (*i.e* upto time t_k).

Note 1: To capture the continuous property of the process model more accurately, higher m should be selected.

Note 2: For $m = 1$, the continuous-discrete filtering algorithm reduces to the ordinary filtering algorithm for discrete-time systems. Hence, the discrete-time filters become a special case of continuous-discrete filters.

C. Update Step

The estimate and covariance of the measurement can be given as

$$\hat{y}_{k|k-1} = \int \gamma(x_k)\aleph(x_k;\hat{x}_{k|k-1}, P_{k|k-1})dx_k \tag{11}$$

$$\begin{aligned}\text{and}\quad P_{yy,k|k-1} &= \int \gamma(x_k)\gamma^T(x_k)\aleph(x_k;\hat{x}_{k|k-1}, P_{k|k-1})dx_k \\ &\quad - \hat{y}_{k|k-1}\hat{y}^T_{k|k-1} + R.\end{aligned} \tag{12}$$

The cross-covariance between the state and the measurement can be given as

$$\begin{aligned}P_{xy,k|k-1} &= \int x_k\gamma^T(x_k)\aleph(x_k;\hat{x}_{k|k-1}, P_{k|k-1})dx_k \\ &\quad - \hat{x}_{k|k-1}\hat{y}^T_{k|k-1}.\end{aligned} \tag{13}$$

On the receipt of a new measurement y_k, the posterior estimate and covariance of the states could be obtained as

$$\hat{x}_{k|k} = \hat{x}_{k|k-1} + K_k(y_k - \hat{y}_{k|k-1}), \tag{14}$$

$$\text{and}\quad P_{k|k} = P_{k|k-1} - K_k P_{yy,k|k-1}K^T_k, \tag{15}$$

where K is Kalman gain, given as

$$K_k = P_{xy,k|k-1}P^{-1}_{yy,k|k-1}. \tag{16}$$

By recursively performing these two steps, the estimates and covariances are computed at every time instant and the filtering of continuous-discrete system is carried out. A complete algorithm diagram for continuous-discrete filtering is provided in Fig. 1.

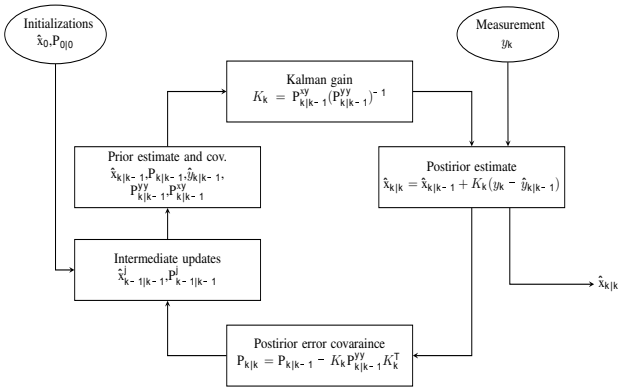

Fig. 1: Algorithm diagram: indicating the steps for filtering of a continuous-discrete system without delay.

The integrals appeared in Eqs. (9)-(13) are intractable for most of the nonlinear structure of f (corresponding f_d) and γ. During filtering, these integrals are computed numerically which gives an approximate solution. Subsequently, the non-linear filters are sub-optimal.

In the Bayesian framework of filtering for continuous-discrete systems, there are mainly two factors which control the accuracy. The first one is the discretization method used for reducing the stochastic ODE to discrete model and another one is the numerical approximation method used for approximating the intractable integrals. In early approaches CD-EKF and CD-UKF, the Euler method is used for discretization. But in CD-CKF, it is replaced by Itô-Taylor expansion of order 1.5 which results in improved accuracy. Also in CD-CKF, the intractable integrals are approximated using the third-degree spherical cubature rule which is most accurate among the methods used in conventional continuous-discrete filtering approaches. Hence, comparing all the available methods, CD-CKF is found to be most promising in terms of accuracy.

IV. Approximation of Multidimensional Integral

The motivation of this work is to develop a more promising continuous-discrete filter by improving the accuracy. To this regard, the conventional CQKF and GHF are enhanced, and the CD-CQKF and the CD-GHF are introduced. In the proposed methods, the Itô-Taylor expansion of order 1.5 is used for deriving the discrete model, like CD-CKF. But to approximate the intractable integrals, the CD-CQKF uses cubature quadrature rule while the CD-GHF uses multidimensional Gauss-Hermite quadrature rule. Both of these rules have better accuracy than the spherical cubature rule used in CD-CKF. Hence, CD-CQKF and CD-GHF is believed to perform with better accuracy compared to the CD-CKF.

A. CD-CQKF

Let us consider $f : R^n \rightarrow R^n$ be a nonlinear function, then the integral of interest appears in the form

$$\begin{aligned} I(f) &= \int_{-\infty}^{\infty} f(x)\aleph(x,\mu,\Sigma)dx \\ &= \frac{1}{\sqrt{\mid \Sigma \mid (2\pi)^n}} \int_{R^n} f(x) e^{-(1/2)(x-\mu)^T \Sigma^{-1}(x-\mu)} dx, \end{aligned} \tag{17}$$

where μ is mean and Σ is covariance matrix. In CD-CQKF, the cubature quadrature rule is used to approximate this integral.

Cubature quadrature rule:

Let us consider that $\lambda_{i'}$ $(i' = 1, 2, \cdots, n')$ are the roots of n' order Chebyshev-Laguerre polynomial equation $L^{\alpha}_{n'}(\lambda)$ $(\alpha = n/2-1)$ [8] being constant and $[u]$ is the set of cubature points lying at the intersection points of unit hyper-sphere and coordinate axes. Then an n'-order cubature quadrature rule states that the integrals of the form $I(f)$ can numerically be approximated with the help of a set of $2nn'$ number of cubature quadrature points ξ_c and their corresponding weight W_c, as follows [8]

$$I(f) \approx \sum_{j=1}^{2nn'} W_{cj} f(\mu + C\xi_{cj}) \tag{18}$$

where

$$\begin{aligned} \xi_{cj} &= \sqrt{2\lambda_{i'}}[u]_i \qquad (i = 1, 2, \cdots 2n), \\ W_{cj} &= \frac{1}{2n\Gamma(n/2)} \times \frac{n'!\Gamma(\alpha + n' + 1)}{\lambda_{i'}[\dot{L}^{\alpha}_{n'}(\lambda_{i'})]^2}. \end{aligned} \tag{19}$$

Using the cubature quadrature rule, the intractable integrals appeared in Eqs. (9)-(13) could be approximated and the filtering is performed. Several remarks on this development are in order:

- The CD-CQKF is free from the *curse of dimensionality* problem as the computational load increases linearly with dimension.
- The CD-CKF is computationally more efficient than the CD-CQKF. But due to the enhanced accuracy, the CD-CQKF can replace CD-CKF.
- The CD-CQKF is a generalized form of CD-CKF. Under the condition of $n' = 1$, it reduces to the CD-CKF.

B. CD-GHF

In CD-GHF, the intractable integrals are approximated using the multidimensional Gauss-Hermite quadrature rule. The conventional Gauss-Hermite quadrature rule is defined for a single dimensional systems while most of the real-life filtering problems are multidimensional. Hence, it is extended to multidimensional rule by using the product rule.

1) Single dimensional Gauss-Hermite quadrature rule: The single dimensional Gauss-Hermite quadrature rule is given by

$$\int_{-\infty}^{\infty} f(\mathrm{x})\aleph(\mathrm{x}; 0, 1)dx = \sum_{i=1}^{N} f(q_i) w_i,$$

where x represents a single dimensional random variable, q_i and w_i are the i^{th} univariate quadrature points and weights associated with it, while N stands for the number of single dimensional (univariate) quadrature points.

To determine the single dimensional quadrature points and weights, let us consider a symmetric tridiagonal matrix J with zero diagonal elements and $J_{i+1,i} = J_{i,i+1} = \sqrt{i/2}; 1 \leq i \leq N-1$. The quadrature points are located at $\sqrt{2}\Psi_i$, where Ψ_i are the eigenvalues of J [16] and the weights w_i are square of the first element of i^{th} normalized vector.

2) Multidimensional Gauss-Hermite quadrature rule: Under the Gaussian assumption of pdfs, the intractable integrals appeared during the filtering are of the form I_f as described in Eq. (17). For a system with zero mean and unity covariance, the same integral appears in the form

$$I_o(f) = \int_{-\infty}^{\infty} f(x)\aleph(x, 0_{n\times 1}, I_n)dx \tag{20}$$

where $0_{n\times 1}$ represents an n-dimensional vector with all the elements as 0 and I_n stands for n-dimensional unity matrix.

The approximation of $I_o(f)$ requires a multidimensional quadrature rule. To this regard, the single dimensional quadrature rule is extended as a multidimensional quadrature rule by applying the product rule. Using this multipldimensional quadrature rule, $I_o(f)$ could be approximated as [16], [20]

$$I_o(f) \approx \sum_{i_1}^{N}\sum_{i_2}^{N}\cdots\sum_{i_n}^{N} f([q_{i_1}, q_{i_2}, \cdots, q_{i_n}]^T) w_{i_1} w_{i_2} \cdots w_{i_n}. \tag{21}$$

Hence, we can write

$$I_o(f) \approx \sum_{j=1}^{N^n} W_{mj} f(\xi_{mj}), \tag{22}$$

where $\xi_{mj} = [q_{i_1}, q_{i_2}, \cdots, q_{i_n}]^T$ is j^{th} multidimensional quadrature point and $W_{mj} = w_{i_1} w_{i_2} \cdots w_{i_n}$ is associated weights.

The above rule could be generalized for arbitrary mean μ and covariance Σ by transforming the multidimensional quadrature points with the same mean and covariance. Hence, the integral $I(f)$ could be approximated as

$$I(f) \approx \sum_{j=1}^{N^n} W_{mj} f(\mu + C\xi_{mj}). \tag{23}$$

Using the multidimensional Gauss-Hermite quadrature rule, the intractable integrals appeared in Eqs. (9)-(13) could be approximated and the filtering is performed.

Few remarks on this development are in order:

- The CD-GHF suffers from the *curse of dimensionality* problem as the computational load increases exponentially with dimension.
- Although the CD-GHF have high computational burden, it can be considered to be superior than the CD-CKF due to improved accuracy.

V. Simulation Results

In this section, the proposed continuous-discrete filters are applied to solve a nonlinear filtering problem of air-traffic-control [15] where the maneuvering trajectory of an aircraft is tracked. The state space equation of the aircraft is given in Eq. (1), where $x = [\epsilon \;\; \dot{\epsilon} \;\; \eta \;\; \dot{\eta} \;\; \zeta \;\; \dot{\zeta} \;\; \omega]^T$ is a seven-dimensional state vector with ϵ, η and ζ representing the radial positions, $\dot{\epsilon}$, $\dot{\eta}$ and $\dot{\zeta}$ representing the velocities in three dimensional X, Y and Z Cartesian coordinates respectively, and ω representing the turn rate. The drift function is given as $f(x) = \begin{bmatrix}\dot{\epsilon} & -\omega\dot{\eta} & \dot{\eta} & \omega\dot{\epsilon} & \dot{\zeta} & 0 & 0\end{bmatrix}^T$, which shows that the motion is horizontal.

To account the modeling errors arising due to wind forces, turbulence *etc.*, a noise vector $\beta(t) = \begin{bmatrix}\beta_1(t) & \beta_2(t) & \cdots & \beta_7(t)\end{bmatrix}^T$ is added. Here, $\beta_i(t)$ is independent of $\beta_j(t)\ \forall\ 1 \leq j \neq i \leq 7$. The diffusion matrix Q is $diag[(0\ \sigma_1^2\ 0\ \sigma_1^2\ 0\ \sigma_1^2\ \sigma_2^2)]^T$.

The motion is severely nonlinear and the extent of nonlinearity depends on the turn rate parameter ω. After applying Itô-Taylor expansion of order 1.5 to Eq. (1), we get the discretized process model as

$$x_k^{j+1} = f_d(x_k^j) + \sqrt{Q}\mathtt{w} + \mathbb{L}f(x_k^j)q, \tag{24}$$

where

$$f_d(x) = \begin{bmatrix} \epsilon + \delta\dot{\epsilon} - \frac{\delta^2}{2}\omega\dot{\eta} \\ \dot{\epsilon} - \delta\omega\dot{\eta} - \frac{\delta^2}{2}\omega^2\dot{\epsilon} - \frac{\delta^2}{2}\sigma_1\sigma_2 \\ \eta + \delta\dot{\eta} + \frac{\delta^2}{2}\omega\dot{\epsilon} \\ \dot{\eta} + \delta\omega\dot{\epsilon} - \frac{\delta^2}{2}\omega^2\dot{\eta} + \frac{\delta^2}{2}\sigma_1\sigma_2 \\ \zeta + \delta\dot{\zeta} \\ \dot{\zeta} \\ \omega \end{bmatrix}$$

and

$$\mathbb{L}f(x) = \begin{bmatrix} 0 & \sigma_1 & 0 & 0 & 0 & 0 & 0 \\ 0 & 0 & 0 & -\sigma_1\omega & 0 & 0 & -\sigma_2\dot{\eta} \\ 0 & 0 & 0 & \sigma_1 & 0 & 0 & 0 \\ 0 & \sigma_1\omega & 0 & 0 & 0 & 0 & \sigma_2\dot{\epsilon} \\ 0 & 0 & 0 & 0 & 0 & \sigma_1 & 0 \\ 0 & 0 & 0 & 0 & 0 & 0 & 0 \\ 0 & 0 & 0 & 0 & 0 & 0 & 0 \end{bmatrix}.$$

The measurements obtained at regular interval of time T is

$$\begin{bmatrix} r_k \\ \theta_k \\ \phi_k \end{bmatrix} = \begin{bmatrix} \sqrt{\epsilon_k^2 + \eta_k^2 + \zeta_k^2} \\ tan^{-1}\left(\frac{\eta_k}{\epsilon_k}\right) \\ tan^{-1}\left(\frac{\zeta_k}{\sqrt{\epsilon_k^2+\eta_k^2}}\right) \end{bmatrix} + v_k.$$

The radar is located at the origin and it is equipped to measure the range r, the azimuth θ and the elevation ϕ. The measurement noise is given as $v_k \sim \aleph(0, R)$ with $R = diag(\begin{bmatrix}\sigma_r^2 & \sigma_\theta^2 & \sigma_\phi^2\end{bmatrix})$, where σ_r, σ_θ and σ_ϕ are standard deviations for range, azimuth and elevation respectively.

For simulation purpose, the initial truth value is considered as $[2000m\ 10m/sec\ 2650m\ 10m/sec\ 200m\ 0m/sec\ \omega^\circ/sec]$. Varying the standard deviation parameters for the noises and the number of iteration per second m, we consider two different scenarios:

scenario 1: $m = 6$, $\sigma_1 = \sqrt{0.2}$, $\sigma_2 = \sqrt{25 \times 10^{-4}}$, $\sigma_r = 70\ m$, $\sigma_\theta = 0.1^o$ and $\sigma_\phi = 0.1^o$.

scenario 2: $m = 10$, $\sigma_1 = \sqrt{0.02}$, $\sigma_2 = \sqrt{25 \times 10^{-5}}$, $\sigma_r = \sqrt{0.1} \times 70\ m$, $\sigma_\theta = \sqrt{0.1} \times 0.1^o$ and $\sigma_\phi = \sqrt{0.1} \times 0.1^o$.

As the height (ζ) and turn rate (ω) are constant, they are initialized in deterministic way. However, the remaining four states are estimated using first two measurements. Hence, the initial estimate could be considered as $\hat{x}_{0|0} = \begin{bmatrix}\epsilon_{m_2} & \frac{\epsilon_{m_2}-\epsilon_{m_1}}{T} & \eta_{m_2} & \frac{\eta_{m_2}-\eta_{m_1}}{T} & 150 & 0 & \omega\end{bmatrix}^T$, where ϵ_{m_k}, η_{m_k}, and ζ_{m_k} are radar measurements in cartesian coordinates at k^{th} time instant given as

$$\epsilon_{m_k} = r_k\ cos\phi_k\ cos\theta_k, \tag{25}$$

$$\eta_{m_k} = r_k\ cos\phi_k\ sin\theta_k, \tag{26}$$

$$\text{and} \quad \zeta_{m_k} = r_k\ sin\phi_k. \tag{27}$$

To derive the initial estimate of error covariance matrix $P_{0|0}$, the methodology discussed in Appendix A and B can be followed.

During the simulation, the second order Gauss-Laguerre quadrature rule ($n' = 2$) is used for the CD-CQKF while 3-points ($N = 3$) univariate quadrature rule is extended to multidimensional rule for implementing the CD-GHF. The simulation is performed for 100 seconds considering a sampling period of $T = 0.5sec$. To compare the results, root mean square error (RMSE) for radial position, velocity and turn rate are calculate at each time step using 500 Monte-Carlo simulations and plotted in Fig. (2) - Fig (5). The plots do not start at the 1^{st} time instant, as this region is under high convergence. From the RMSE plots, it could be concluded that the proposed methods *i.e.* CD-CQKF and CD-GHF could provide better accuracy than the CD-CKF which is most accurate filter available in literature to deal with the continuous-discrete filtering problems. However, relative computational time analysis in Table I indicates comparatively high computational burden for the proposed methods, especially for the CD-GHF.

The purpose of performance analysis is to compare the improvement caused due to enhancing numerical the high

accuracy discrete-time filters in continuous-discrete domain. In this regard, the CD-EKF and the CD-UKF have been excluded from the comparison as they utilize Itô-Taylor expansion of order 0.5 that may be an extended reason for comparatively poor estimation accuracy.

TABLE I: Relative computational time for CD filters

CD filter	Relative computational time
CD-CKF	1
CD-CQKF	1.6
CD-GHF	255.6

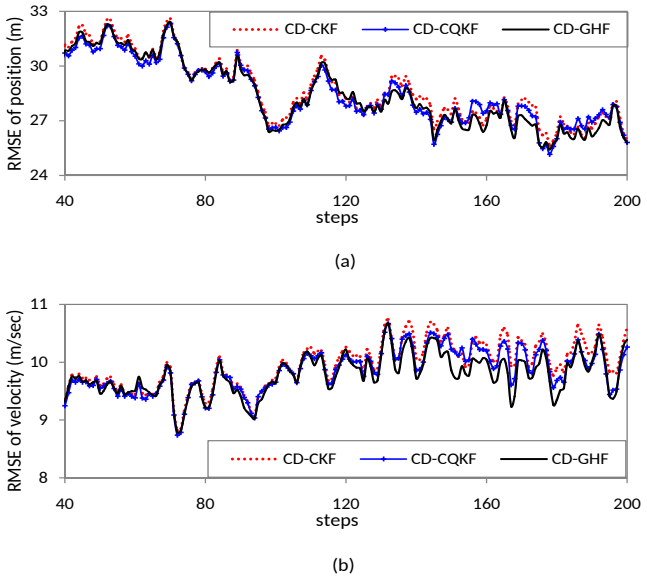

Fig. 2: *scenario 1*: RMSE plots for $\omega = 3^\circ/sec$ (a) position in m, (b) velocity in m/sec.

VI. Discussions and Conclusions

The widely arising continuous-discrete filtering problems concerning to the fields of tracking and navigation impels to develop an accurate and computationally efficient solution. In this paper, the conventional CQKF and GHF are extended and, the CD-CQKF and the CD-GHF are introduced to deal with such problems. In the proposed methods, the continuous process model is first reduced to an ODE from which a discrete model is obtained using the Itô-Taylor expansion of order 1.5. The Itô-Taylor expansion of order 1.5 is most accurate method available in filtering literature and also used in CD-CKF. In proposed methods, further accuracy could be enhanced by replacing the third degree spherical cubature rule used in CD-CKF for approximating the intractable integrals appeared during the filtering. In CD-CQKF, this approximation is performed using cubature quadrature rule while CD-GHF uses multidimensional Gauss-Hermite quadrature rule for the same.

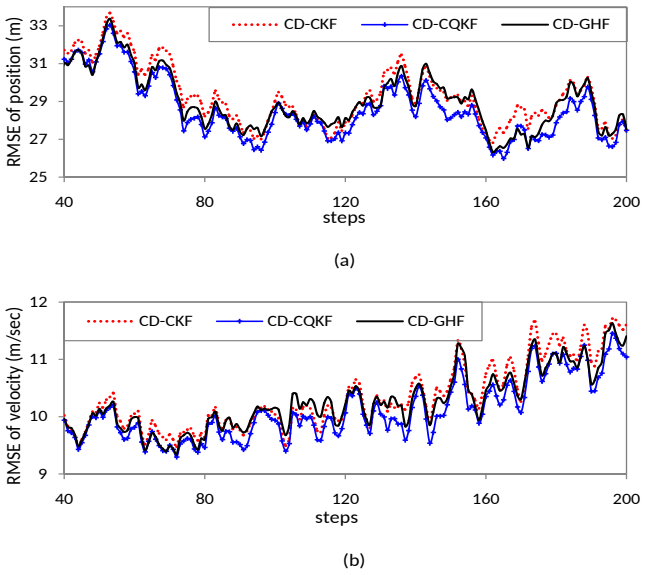

Fig. 3: *scenario 1*: RMSE plots for $\omega = 4.5^\circ/sec$ (a) position in m, (b) velocity in m/sec.

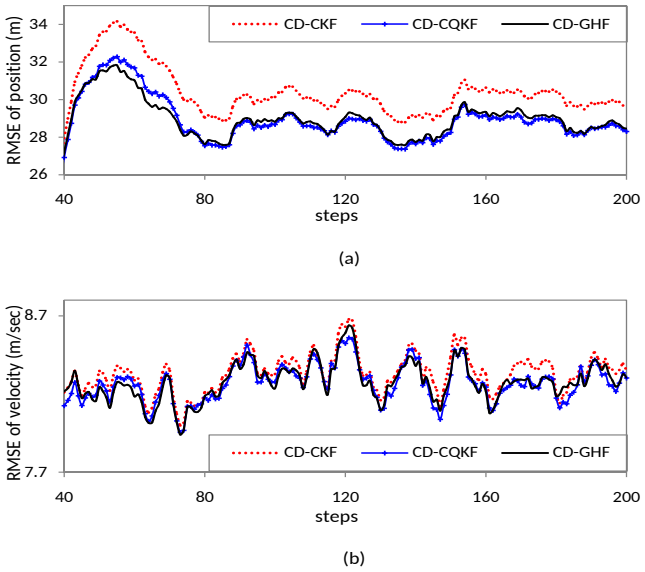

Fig. 4: *scenario 2*: RMSE plots for $\omega = 3^\circ/sec$ (a) position in m, (b) velocity in m/sec.

The performance of the proposed CD-CQKF and the CD-GHF are compared with the CD-CKF and it is found that the accuracy of the proposed methods are better. Due to the enhanced accuracy, the proposed filters can replace the conventional methods available in literature.

Appendix

A. Derivation of initial error covariance $\boldsymbol{P}_{0|0}$

Let us consider

$$\epsilon_{mk} = \epsilon_k + v_{\epsilon k}, \quad \eta_{mk} = \eta_k + v_{\eta k}, \quad \text{and,} \quad \zeta_{mk} = \zeta_k + v_{\zeta k} \tag{28}$$

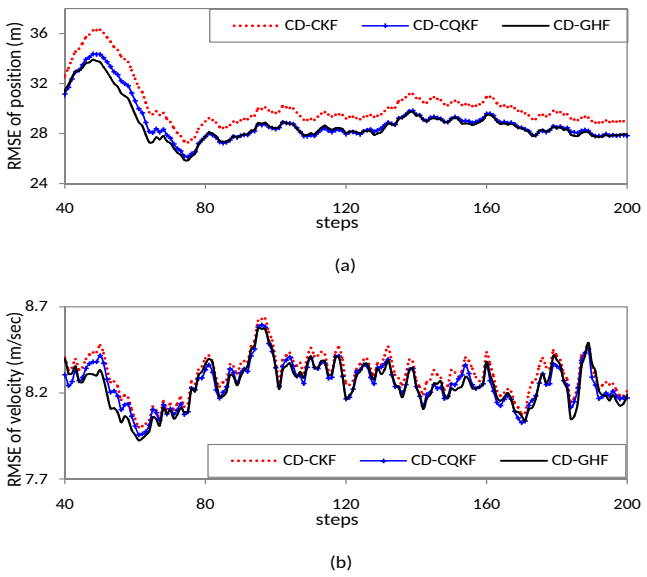

Fig. 5: *scenario 2*: RMSE plots for $\omega = 4.5^\circ/sec$ (a) position in m, (b) velocity in m/sec.

where ϵ_k, η_k and ζ_k are truth values, ϵ_{mk}, η_{mk} and ζ_{mk} are measurement values and $v_{\epsilon k}$, $v_{\eta k}$ and $v_{\zeta k}$ are measurement noises at k^{th} time instant in Cartesian coordinates.

Similarly,

$$r_k = r'_k + v_{rk}, \quad \theta_k = \theta'_k + v_{\theta k}, \quad \text{and,} \quad \phi_k = \phi'_k + v_{\phi k} \tag{29}$$

where r'_k, θ'_k and ϕ'_k are truth values, r_k, θ_k and ϕ_k are measured values and v_{rk}, $v_{\theta k}$ and $v_{\phi k}$ are measurement noises at k^{th} time instant associated with radar range, azimuth and elevation respectively.

The filter is initialized from the first two measurements as

$$\hat{x}_{0|0} = \left[\epsilon_{m2} \;\; \frac{\epsilon_{m2}-\epsilon_{m1}}{T} \;\; \eta_{m2} \;\; \frac{\eta_{m2}-\eta_{m1}}{T} \;\; \zeta_{m2} \;\; \frac{\zeta_{m2}-\zeta_{m1}}{T} \;\; \frac{\theta_2-\theta_1}{T}\right]^T.$$

The initial value of truth is given as $x_0 = \left[\epsilon_2 \;\; \frac{\epsilon_2-\epsilon_1}{T} \;\; \eta_{m2} \;\; \frac{\eta_2-\eta_1}{T} \;\; \zeta_{m2} \;\; \frac{\zeta_2-\zeta_1}{T} \;\; \frac{\theta'_2-\theta'_1}{T}\right]^T$. The initial error covariance $P_{0|0}$ is given as $P_{0|0} = \mathbb{E}[\,\hat{e}_{0|0}\,\hat{e}^T_{0|0}]$ where the initial error is given as (from Eqs. (28)-(29))

$$\begin{aligned}\hat{e}_{0|0} &= \hat{x}_{0|0} - x_0 \\ &= \left[v_{\epsilon 2} \;\; \frac{v_{\epsilon 2}-v_{\epsilon 1}}{T} \;\; v_{\eta 2} \;\; \frac{v_{\eta 2}-v_{\eta 1}}{T} \;\; v_{\zeta 2} \;\; \frac{v_{\zeta 2}-v_{\zeta 1}}{T} \;\; \frac{v_{\theta 2}-v_{\theta 1}}{T}\right].\end{aligned}$$

Here, $v_{\epsilon k} \sim \aleph(0, \sigma^2_\epsilon)$, $v_{\eta k} \sim \aleph(0, \sigma^2_\eta)$ and $v_{\zeta k} \sim \aleph(0, \sigma^2_\zeta)$ are white Gaussian noises with zero mean. So, to get the expression for $P_{0|0}$, let us consider $\mathbb{E}[v_{\epsilon i} v_{\epsilon j}] = \sigma^2_\epsilon \delta_{ij}$, $\mathbb{E}[v_{\eta i} v_{\eta j}] = \sigma^2_\eta \delta_{ij}$ and $\mathbb{E}[v_{\zeta i} v_{\zeta j}] = \sigma^2_\zeta \delta_{ij}$, and $\mathbb{E}[v_{\epsilon i} v_{\eta j}] = \sigma_{\epsilon\eta}\delta_{ij}$, $\mathbb{E}[v_{\epsilon i} v_{\zeta j}] = \sigma_{\epsilon\zeta}\delta_{ij}$ and $\mathbb{E}[v_{\eta i} v_{\zeta j}] = \sigma_{\eta\zeta}\delta_{ij}$ (where δ_{ij} is Kronecker delta function). Also, since $v_{\theta k} \sim \aleph(0, \sigma^2_\theta)$ is white noise, we put $\mathbb{E}[v_{\theta i} v_{\theta j}] = \sigma^2_\theta \delta_{ij}$. So the expression for $P_{0|0}$ can be given as

$$P_{0|0} = \begin{bmatrix} \sigma^2_\epsilon & \frac{\sigma^2_\epsilon}{T} & \sigma_{\epsilon\eta} & \frac{\sigma_{\epsilon\eta}}{T} & \sigma_{\epsilon\zeta} & \frac{\sigma_{\epsilon\zeta}}{T} & 0 \\ \frac{\sigma^2_\epsilon}{T} & \frac{2\sigma^2_\epsilon}{T^2} & \frac{\sigma_{\epsilon\eta}}{T} & \frac{2\sigma_{\epsilon\eta}}{T^2} & \frac{\sigma_{\epsilon\zeta}}{T} & \frac{2\sigma_{\epsilon\zeta}}{T^2} & 0 \\ \sigma_{\epsilon\eta} & \frac{\sigma_{\epsilon\eta}}{T} & \sigma^2_\eta & \frac{\sigma^2_\eta}{T} & \sigma_{\eta\zeta} & \frac{\sigma_{\eta\zeta}}{T} & 0 \\ \frac{\sigma_{\epsilon\eta}}{T} & \frac{2\sigma_{\epsilon\eta}}{T^2} & \frac{\sigma^2_\eta}{T} & \frac{2\sigma^2_\eta}{T^2} & \frac{\sigma_{\eta\zeta}}{T} & \frac{2\sigma_{\eta\zeta}}{T^2} & 0 \\ \sigma_{\epsilon\zeta} & \frac{\sigma_{\epsilon\zeta}}{T} & \sigma_{\eta\zeta} & \frac{\sigma_{\eta\zeta}}{T} & \sigma^2_\zeta & \frac{\sigma^2_\zeta}{T} & 0 \\ \frac{\sigma_{\epsilon\zeta}}{T} & \frac{2\sigma_{\epsilon\zeta}}{T^2} & \frac{\sigma_{\eta\zeta}}{T} & \frac{2\sigma_{\eta\zeta}}{T^2} & \frac{\sigma^2_\zeta}{T} & \frac{2\sigma^2_\zeta}{T^2} & 0 \\ 0 & 0 & 0 & 0 & 0 & 0 & \frac{2\sigma^2_\theta}{T^2} \end{bmatrix}.$$

B. Derivation of measurement noise covariance R_k in Cartesian coordinate

Substituting Eqs. (25)-(27) in Eq. (28), we get

$$r_k \; cos \; \phi_k \; cos \; \theta_k = \epsilon_k + v_{\epsilon k}, \tag{30}$$

$$r_k \; cos \; \phi_k \; sin \; \theta_k = \eta_k + v_{\eta k}, \tag{31}$$

$$\text{and,} \quad r_k \; sin \; \phi_k = \zeta_k + v_{\zeta k}. \tag{32}$$

Similarly, substituting Eq. (29) into Eq. (30) to Eq. (32), we get

$$(r'_k + v_{rk}) \; cos \; (\phi'_k + v_{\phi k}) \; cos \; (\theta'_k + v_{\theta k}) = \epsilon_k + v_{\epsilon k}, \tag{33}$$

$$(r'_k + v_{rk}) \; cos \; (\phi'_k + v_{\phi k}) \; sin \; (\theta'_k + v_{\theta k}) = \eta_k + v_{\eta k}, \tag{34}$$

$$\text{and} \quad (r'_k + v_{rk}) \; sin \; (\phi'_k + v_{\phi k}) = \zeta_k + v_{\zeta k}. \tag{35}$$

From Eq. (33)

$$\begin{aligned}(r'_k + v_{rk})(cos \; \phi'_k \; cos \; v_{\phi k} - sin \; \phi'_k \; sin \; v_{\phi k})(cos \; \theta'_k \; cos \; v_{\theta k} \\ - sin \; \theta'_k \; sin \; v_{\theta k}) = \epsilon_k + v_{\epsilon k}.\end{aligned} \tag{36}$$

Since, $v_{rk} \sim \aleph(0, \sigma^2_r)$, $v_{\theta k} \sim \aleph(0, \sigma^2_\theta)$ and $v_{\phi k} \sim \aleph(0, \sigma^2_\phi)$, so assuming $v_{\phi k} \to 0 \;\; \Rightarrow cos \; v_{\phi k} \to 1 \;\; \Rightarrow sin \; v_{\phi k} \to v_{\phi k}$ and, $v_{\theta k} \to 0 \;\; \Rightarrow cos \; v_{\theta k} \to 1 \;\; \Rightarrow sin \; v_{\theta k} \to v_{\theta k}$ Eq. (36) reduces to

$$\begin{aligned}(r'_k + v_{rk})(cos \; \phi'_k - v_{\phi k} \; sin \; \phi'_k)(cos \; \theta'_k - v_{\theta k} \; sin \; \theta'_k) \\ = \epsilon_k + v_{\epsilon k}\end{aligned}$$

$$\begin{aligned}\Rightarrow (r'_k + v_{rk})(cos \; \phi'_k \; cos \; \theta'_k - v_{\theta k} \; sin \; \theta'_k \; cos \; \phi'_k \\ - v_{\phi k} \; sin \; \phi'_k \; cos \; \theta'_k + v_{\phi k} \; v_{\theta k} \; sin \; \phi'_k \; sin \; \theta'_k) = \epsilon_k + v_{\epsilon k}.\end{aligned}$$

Assuming $v_{\theta k} \; v_{\phi k} \to 0$, $v_{rk} \; v_{\phi k} \to 0$ and $v_{rk} \; v_{\theta k} \to 0$, we get

$$\begin{aligned}r'_k cos \; \phi'_k \; cos \; \theta'_k - r'_k \; v_{\theta k} \; sin \; \theta'_k \; cos \; \phi'_k - r'_k \; v_{\phi k} \; sin \; \phi'_k \; cos \; \theta'_k \\ + v_{rk} \; cos \; \phi'_k \; cos \; \theta'_k = \epsilon_k + v_{\epsilon k}.\end{aligned}$$

Since $\epsilon_k = r'_k \; cos \; \phi'_k \; cos \; \theta'_k$, hence

$$\begin{aligned}v_{\epsilon k} = & v_{rk} \; cos \; \phi'_k \; cos \; \theta'_k - r'_k \; v_{\theta k} \; sin \; \theta'_k \; cos \; \phi'_k \\ & - r'_k \; v_{\phi k} \; sin \; \phi'_k \; cos \; \theta'_k.\end{aligned} \tag{37}$$

Now, from Eq. (34)

$$\begin{aligned}(r'_k + v_{rk})(cos \; \phi'_k \; cos \; v_{\phi k} - sin \; \phi'_k \; sin \; v_{\phi k})(sin \; \theta'_k \; cos \; v_{\theta k} \\ + cos \; \theta'_k \; sin \; v_{\theta k}) = \eta_k + v_{\eta k}.\end{aligned} \tag{38}$$

Since $v_{rk} \sim \aleph(0, \sigma_r^2)$, $v_{\theta k} \sim \aleph(0, \sigma_\theta^2)$ and $v_{\phi k} \sim \aleph(0, \sigma_\phi^2)$, so assuming $v_{\phi k} \to 0 \quad \Rightarrow cos\ v_{\phi k} \to 1 \quad \Rightarrow sin\ v_{\phi k} \to v_{\phi k}$ and, $v_{\theta k} \to 0 \quad \Rightarrow cos\ v_{\theta k} \to 1 \quad \Rightarrow sin\ v_{\theta k} \to v_{\theta k}$, Eq. (38) reduces to

$$(r'_k + v_{rk})(cos\ \phi'_k - v_{\phi k}\ sin\ \phi'_k)(sin\ \theta'_k + cos\ \theta'_k\ \ v_{\theta k}) = \eta_k + v_{\eta k}$$

$$\Rightarrow (r'_k + v_{rk})(cos\ \phi'_k\ sin\ \theta'_k + v_{\theta k}\ cos\ \phi'_k\ cos\ \theta'_k - v_{\phi k}\ sin\ \phi'_k\ sin\ \theta'_k - v_{\phi k}\ v_{\theta k}\ sin\ \phi'_k\ cos\ \theta'_k) = \eta_k + v_{\eta k}.$$

Assuming $v_{\theta k}\ v_{\phi k} \to 0$, $v_{rk}\ v_{\phi k} \to 0$ and $v_{rk}\ v_{\theta k} \to 0$, we get

$$r'_k\ cos\ \phi'_k\ sin\ \theta'_k + r'_k\ v_{\theta k}\ cos\ \phi'_k\ cos\ \theta'_k - r'_k\ v_{\phi k}\ sin\ \phi'_k\ sin\ \theta'_k + v_{rk}\ cos\ \phi'_k\ sin\ \theta'_k = \eta_k + v_{\eta k}.$$

Since $\eta_k = r'_k\ cos\ \phi'_k\ sin\ \theta'_k$, hence

$$\begin{aligned} v_{\eta k} =& v_{rk}\ cos\ \phi'_k\ sin\ \theta'_k + r'_k\ v_{\theta k}\ cos\ \phi'_k\ cos\ \theta'_k \\ & - r'_k\ v_{\phi k}\ sin\ \phi'_k\ sin\ \theta'_k. \end{aligned} \tag{39}$$

From Eq. (35)

$$(r'_k + v_{rk})\ (sin\ \phi'_k\ cos\ v_{\phi k} + cos\ \phi'_k\ sin\ v_{\phi k}) = \zeta_k + v_{\zeta k}.$$

Assuming $v_{\phi k} \to 0 \quad \Rightarrow cos\ v_{\phi k} \to 1 \quad \Rightarrow sin\ v_{\phi k} \to v_{\phi k}$, we get

$$(r'_k + v_{rk})\ (sin\ \phi'_k + v_{\phi k}\ cos\ \phi'_k) = \zeta_k + v_{\zeta k}. \tag{40}$$

Assuming $v_{rk}\ v_{\phi k} \to 0$, we get

$$r'_k\ sin\ \phi'_k + r'_k\ v_{\phi k}\ cos\ \phi'_k + v_{rk}\ sin\ \phi'_k = \zeta_k + v_{\zeta k}. \tag{41}$$

Since $\zeta_k = r'_k\ sin\ \phi'_k$,we get

$$v_{\zeta k} = r'_k\ v_{\phi k}\ cos\ \phi'_k + v_{rk}\ sin\ \phi'_k. \tag{42}$$

From Eq. (37), Eq. (39) and Eq. (42), the measurement noise vector in Cartesian coordinate is given as

$$\begin{aligned} V_k =& \begin{bmatrix} v_{\epsilon k} & v_{\eta k} & v_{\zeta k} \end{bmatrix}^T \\ =& \begin{bmatrix} v_{rk}cos\phi'_k cos\theta'_k - r'_k v_{\theta k} sin\theta'_k cos\phi'_k - r'_k v_{\phi_k} sin\phi'_k cos\theta'_k \\ v_{rk}cos\phi'_k sin\theta'_k + r'_k v_{\theta k} cos\phi'_k cos\theta'_k - r'_k v_{\phi k} sin\phi'_k sin\theta'_k \\ r'_k v_{\phi k} cos\phi'_k + v_{rk} sin\phi'_k \end{bmatrix} \end{aligned}$$

The measurement noise covariance R_k in cartesian coordinate is given by

$$R_k = \mathbb{E}[V_k V_k^T] = \mathbb{E}\left(\begin{bmatrix} v_{\epsilon k} & v_{\eta k} & v_{\zeta k} \end{bmatrix}^T \begin{bmatrix} v_{\epsilon k} & v_{\eta k} & v_{\zeta k} \end{bmatrix} \right).$$

Since $v_{rk} \sim \aleph(0, \sigma_r^2)$, $v_{\phi k} \sim \aleph(0, \sigma_\phi^2)$ and $v_{\theta k} \sim \aleph(0, \sigma_\theta^2)$ are white Gaussian noises with zero mean and are independent from each other, so putting $\mathbb{E}[v_{rk} v_{rk}] = \sigma_r^2$, $\mathbb{E}[v_{\phi k} v_{\phi k}] = \sigma_\phi^2$, $\mathbb{E}[v_{\theta k} v_{\theta k}] = \sigma_{\theta k}^2$ and $\mathbb{E}[v_{rk} v_{\phi k}] = 0$, $\mathbb{E}[v_{rk} v_{\theta k}] = 0$ and $\mathbb{E}[v_{\phi k} v_{\theta k}] = 0$, we get

$$R_k = \begin{bmatrix} R_{11k} & R_{12k} & R_{13k} \\ R_{21k} & R_{22k} & R_{23k} \\ R_{31k} & R_{32k} & R_{33k} \end{bmatrix} = \begin{bmatrix} \sigma_\epsilon^2 & \sigma_{\epsilon\eta} & \sigma_{\epsilon\zeta} \\ \sigma_{\epsilon\eta} & \sigma_\eta^2 & \sigma_{\eta\zeta} \\ \sigma_{\epsilon\zeta} & \sigma_{\eta\zeta} & \sigma_\zeta^2 \end{bmatrix}, \tag{43}$$

where

$$\begin{aligned} \sigma_\epsilon^2 =& \sigma_r^2\ cos^2\ \phi'_k\ cos^2\ \theta'_k + r_k'^2\ \sigma_\theta^2\ cos^2\ \phi'_k\ sin^2\ \theta'_k \\ & + r_k'^2\ \sigma_\phi^2\ sin^2\ \phi'_k\ cos^2\ \theta'_k, \end{aligned}$$

$$\begin{aligned} \sigma_{\epsilon\eta} =& \sigma_r^2\ cos^2\ \phi'_k\ cos\ \theta'_k\ sin\ \theta'_k - r_k'^2\ \sigma_\theta^2\ cos^2\ \phi'_k\ sin\ \theta'_k\ cos\ \theta'_k \\ & + r_k'^2\ \sigma_\phi^2\ sin^2\ \phi'_k\ cos\ \theta'_k\ sin\ \theta'_k, \end{aligned}$$

$$\sigma_{\epsilon\zeta} = \sigma_r^2\ cos\ \phi'_k\ sin\ \phi'_k\ cos\ \theta'_k - r_k'^2\ \sigma_\phi^2\ cos\ \phi'_k\ sin\ \phi'_k\ cos\ \theta'_k,$$

$$\begin{aligned} \sigma_\eta^2 =& \sigma_r^2\ cos^2\ \phi'_k\ sin^2\ \theta'_k + r_k'^2\ \sigma_\theta^2\ cos^2\ \phi'_k\ cos^2\ \theta'_k \\ & + r_k'^2\ \sigma_\phi^2\ sin^2\ \phi'_k\ sin^2\ \theta'_k, \end{aligned}$$

$$\sigma_{\eta\zeta} = \sigma_r^2\ cos\ \phi'_k\ sin\ \phi'_k\ sin\ \theta'_k - r_k'^2\ \sigma_\phi^2\ cos\ \phi'_k\ sin\ \phi'_k\ sin\ \theta'_k,$$

$$\text{and} \quad \sigma_\zeta^2 = \sigma_r^2\ sin^2\ \phi'_k + r_k'^2\ \sigma_\phi^2\ cos^2\ \phi'_k.$$

REFERENCES

[1] Y. Bar-Shalom, X. R. Li, and T. Kirubarajan, *Estimation with applications to tracking and navigation: theory algorithms and software*. John Wiley & Sons, 2004.

[2] Y. Hongpeng, P. Chao, C. Yi, and F. Qu, "A robust object tracking algorithm based on surf and kalman filter," *Intelligent Automation & Soft Computing*, vol. 19, no. 4, pp. 567–579, 2013.

[3] Y.-C. Chou and M. Nakajima, "Particle filter planar target tracking with a monocular camera for mobile robots," *Intelligent Automation & Soft Computing*, vol. 23, no. 1, pp. 117–125, 2017.

[4] M. S. Grewal, L. R. Weill, and A. P. Andrews, *Global positioning systems, inertial navigation, and integration*. John Wiley & Sons, 2007.

[5] J. R. Raol and N. K. Sinha, "Advances in modelling, system identification and parameter estimation," *Sadhana*, vol. 25, no. 2, pp. 71–73, 2000.

[6] S. Julier, J. Uhlmann, and H. F. Durrant-Whyte, "A new method for the nonlinear transformation of means and covariances in filters and estimators," *IEEE Transactions on automatic control*, vol. 45, no. 3, pp. 477–482, 2000.

[7] I. Arasaratnam and S. Haykin, "Cubature Kalman filters," *IEEE Transactions on automatic control*, vol. 54, no. 6, pp. 1254–1269, 2009.

[8] S. Bhaumik *et al.*, "Cubature quadrature Kalman filter," *IET Signal Processing*, vol. 7, no. 7, pp. 533–541, 2013.

[9] B. Jia, M. Xin, and Y. Cheng, "High-degree cubature Kalman filter," *Automatica*, vol. 49, no. 2, pp. 510–518, 2013.

[10] A. K. Singh and S. Bhaumik, "Higher degree cubature quadrature Kalman filter," *International Journal of Control, Automation and Systems*, vol. 13, no. 5, pp. 1097–1105, 2015.

[11] W. H. Fleming and W. M. McEneaney, "Robust limits of risk sensitive nonlinear filters," *Mathematics of Control, Signals and Systems*, vol. 14, no. 2, pp. 109–142, 2001.

[12] A. H. Jazwinski, *Stochastic processes and filtering theory*. Courier Corporation, 2007.

[13] J. B. Jorgensen, P. G. Thomsen, H. Madsen, and M. R. Kristensen, "A computationally efficient and robust implementation of the continuous-discrete extended Kalman filter," in *American Control Conference, 2007. ACC'07*. IEEE, 2007, pp. 3706–3712.

[14] S. Sarkka, "On unscented Kalman filtering for state estimation of continuous-time nonlinear systems," *IEEE Transactions on automatic control*, vol. 52, no. 9, pp. 1631–1641, 2007.

[15] I. Arasaratnam, S. Haykin, and T. R. Hurd, "Cubature Kalman filtering for continuous-discrete systems: theory and simulations," *IEEE Transactions on Signal Processing*, vol. 58, no. 10, pp. 4977–4993, 2010.

[16] I. Arasaratnam, S. Haykin, and R. J. Elliott, "Discrete-time nonlinear filtering algorithms using gauss–hermite quadrature," *Proceedings of the IEEE*, vol. 95, no. 5, pp. 953–977, 2007.

[17] A. K. Singh and S. Bhaumik, "Nonlinear estimation using transformed gauss-hermite quadrature points," in *Signal Processing, Computing and Control (ISPCC), 2013 IEEE International Conference on*. IEEE, 2013, pp. 1–4.

[18] B. Jia, M. Xin, and Y. Cheng, "Sparse-grid quadrature nonlinear filtering," *Automatica*, vol. 48, no. 2, pp. 327–341, 2012.

[19] A. K. Singh and S. Bhaumik, "Quadrature filters for maneuvering target tracking," in *Recent Advances and Innovations in Engineering (ICRAIE), 2014*. IEEE, 2014, pp. 1–6.

[20] K. Ito and K. Xiong, "Gaussian filters for nonlinear filtering problems," *IEEE transactions on automatic control*, vol. 45, no. 5, pp. 910–927, 2000.